Multiphysics Simulation of REMS hot-film Anemometer Under Typical Martian Atmosphere Conditions

Lukasz Kowalski[*1], Luis Castañer Muñoz[1], Manuel Domínguez Pumar[1], Vicente Jiménez Serres[1]

[*]Corresponding author: Jordi Girona 1-3, 08034 Barcelona, Spain; tel.: (+34) 934016766, lukasz@eel.upc.edu
[1]Universitat Politècnica de Catalunya (UPC http://www.upc.edu), Departament d'Enginyeria Electrònica (DEE http://www-eel.upc.edu), Micro and Nano Technologies Research Group (MNT http://webmnt.upc.es)

Abstract: The purpose of this paper is to describe numerical electro-thermal simulations of the REMS wind sensor unit [3] and the results obtained by using COMSOL multiphysics. This device is a hot-film anemometer for 2D wind measurements, which does not have movable parts and is based on the air stream forced heat convection to the environment. This wind sensor works as a thermo-electrical transducer where the same equilibrium temperature is reached for every value of the wind speed, by means of a power supply modulations. Therefore, the straightforward relationship between the amount of power delivered to the unit and the wind speed can be derived as earlier presented [2]. Detailed finite element simulations enabled us to predict the temperature distribution, recognize hot and cold spots and characterize besides the thermal profile the operating sensing magnitudes.

Keywords: hot anemometry, heat convection, thermal profile, temperature distribution, REMS.

1. Introduction

In the fall 2011 Jet Propulsion Laboratory (JPL) is planning to launch Mars Science Laboratory (MSL) rover equipped with Rover Environmental Monitoring Station (REMS) to perform meteorological test on the surface of the Mars. More details about Spanish contribution to this particular NASA mission can be found in [1]. One of the meteorological devices on board of the MSL Rover is a small thermo-electric transducer designed at UPC. It will be exposed to the harsh weather conditions on the 'Red Planet' in order to characterize wind fluxes occurring in the proximity of the ground. The sensor chip has been extensively described earlier [3, 4]. This chip is the heart of the wind sensor - thermal anemometer working in the constant temperature difference to ambient mode. It has been found in [5] that the uniformity of the temperature distribution on the external surface of the sensor die, which is in contact with the ambient, is highly desirable for proper functionality of the device, especially in a rarified atmosphere where the wind-related heat exchange is considerably attenuated.

1.1 Mars atmosphere

There is a significant difference in Martian typical atmosphere conditions in comparison to the terrestrial atmosphere, as shown in table 1.

Table 1: Earth vs. Mars atmosphere

Parameter	Earth	Mars
Average temp.	300K	220K
Temp. variation	200K-350K	150K-300K
Ambient pressure	1013hPa	6-8hPa
Atmosphere composition	N_2 - 78.0% O_2 - 20.9% Ar - 0.9%	CO_2 - 95.3% N_2 - 2.7% Ar - 1.6%

The shallow atmosphere and low temperatures with high diurnal variation are the key challenges that a wind sensor faces for this application.

2. Sensor unit structure

The sensor unit is made of a silicon oxidized die – chip of a size $1.6\text{mm} \times 1.6\text{mm} \times 0.4\text{mm}$ on which an 80nm thick platinum film is sputtered and patterned. The chip is supported by a pyrex inverted table structure which also thermally isolates the silicon die from the PCB substrate. The platinum resistors that come out of the patterning are terminated in gold pads that are bonded with gold wires to the electrical terminals located on the PCB base, as seen in figure 1.

3. Heat transfer theory

From the functional point of view, the sensor governing equation can be written by setting the power equilibrium in a stationary state:

$$P_{gen} = P_{cond} + P_{conv}$$

, where: P_{gen} is the heat power generated by Joule effect in the platinum resistor, P_{cond} is the power losses by heat conduction trough the pyrex support and the wire-bonding itself, P_{conv} is the power convection from the overheated silicon die surface, enhanced by the wind speed.

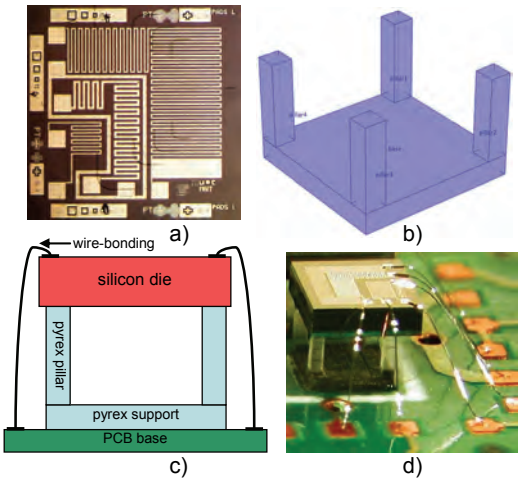

Figure 1. Sensor unit; a) platinum pattern on the silicon die surface, b) pyrex support c) drawing of a sensor unit assembled on PCB and wired with gold bonding, d) photo of the entire assembled unit.

3.1 Joule heat generation

An electrical current I flowing through the fraction of the resistive element ΔR generates power heat ΔP_{gen} according to the Joule law:

$$\Delta P_{gen} = I^2 \cdot \Delta R$$

Since resistive element in this particular case of wind sensor is a platinum strip, therefore, the fractional resistance is related to its dimensions and to the platinum electrical resistivity ρ_{Pt} as:

$$\Delta R = \frac{\Delta L_{Pt} \cdot \rho_{Pt}}{W_{Pt} \cdot H_{Pt}}$$

, where: ΔL_{Pt} -length, W_{Pt} -width, H_{Pt} -height of the resistive element. As well, the electrical resistivity of the platinum material can be modeled by a lineal function of the temperature with a positive temperature coefficient - α_{Pt} , so:

$$\rho_{Pt(T[K])} = \rho_{Pt(273K)} \cdot \left(1 + \alpha_{Pt} \cdot T\right)$$

, where: $\rho_{Pt(273K)}$ is the platinum electrical resistivity at reference temperature 273K and T is the temperature in Kelvin scale. Hence, power generation equation can be developed into form:

$$\Delta P_{gen} = I^2 \cdot \frac{\Delta L_{Pt} \cdot \rho_{Pt(273K)}}{W_{Pt} \cdot H_{Pt}} \cdot \left(1 + \alpha_{Pt} \cdot T\right)$$

3.2 Power conduction

The heat flow which can be associated with power heat conduction depends on the thermal properties of the material and on the temperature gradient along the material:

$$\Delta P_{cond} = -k \cdot A_{cross} \cdot \frac{\Delta T}{\Delta x}$$

, where: A_{cross} is the across section of the heat volume, ΔT is a temperature difference on the ends of terminal which length is Δx and k is the thermal conductivity coefficient of material.

3.3 Power convection

Power convection from the hot element to the ambient is a function of the heat transfer coefficient h, contact surface $A_{contact}$ and the temperature difference ΔT between hot surface T_{hot} and air T_{air} and can be described as follow:

$$\Delta P_{conv} = h \cdot A_{contact} \cdot \Delta T$$

, where: the temperature difference is simply:

$$\Delta T = T_{hot} - T_{air}$$

Table 2: Material properties used in FEM simulation

Parameter	**Si**	**Pt**	**Ag**	**Pyrex**
Element	die	paths	pads, wire	table
k-thermal conductivity, W/mK	149	71.6	318	1.1
Cp–heat Capacity, J/kgK	710	130	235	750
ρ-density ,Kg/m^3	2329	21450	10490	2230
γ- resistivity, Ωm	-	105e-9	15,8e-9	-
α-temperature coefficient, 1/K	-	3,85e-3	0	-

4. Use of COMSOL Multiphysics

The specific values we have used for the physical properties are gathered in table 2. In order to satisfy multiphysics problem, where electrical and thermal domain are mixed each other two different physics has been proposed with carefully assigned boundary conditions.

4.1 Conductive media DC (dc) domain

In this simulation domain only platinum resistance R_{heat}, with two gold pads have been included. The entire path is electrically isolated and the top surface of the one pad is assigned to ground potential whereas the second pad top surface is connected to an electrical current of nominal value of 5mA**.** Constant current is used to simplify constant temperature conditions and to satisfy available boundary conditions this value is translated into current density J_{heater} as:

$$J_{heater} = \frac{I_{heater}}{S_{pad}} = \frac{5mA}{(150 \cdot \mu m)^2} = 222\,kA/m^2$$

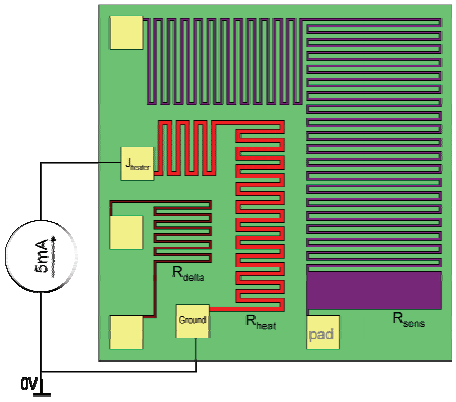

Figure 2. External DC current source connection with platinum heater resistance together with indication of ground reference pad and fixed current density pad.

4.2 Heat transfer by conduction (ht) domain

All components of the sensor have been included into this particular simulation domain. The only heat source is the platinum heater resistance and all the heat comes from the Joule effect simulated in conductive media DC domain. Fixed temperature boundary condition of 280K has been set up for the surface which connects the pyrex support with the PCB base. The same temperature 280K has been assigned to the surrounding air and for all surface in contact with the ambient air the boundary condition-convection coefficient has been set for 5W/m^{2}K. Although the simulation model does not have physical representation of the wire-bonding connections as presented in figure 3, their heat conduction capacity is taken under consideration.

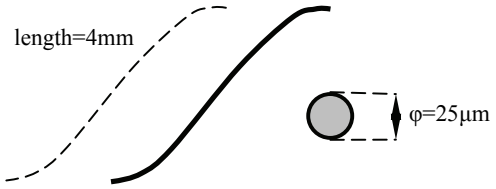

Figure 3. Single wire-bonding.

For every single wire, the conduction power can be calculated from the following equation:

$$P_{cond.wire} = -k_{pyrex} \cdot \frac{A_{cross.wire}}{L_{wire}} \cdot (T_{hot} - T_{PCB})\mathrm{L}$$

et us now assume that $P_{cond.wire}$ which is the power conduction by wire can be modeled by an additional convection $P_{conv.add}$ term occurring only on the surface of the pads:

$$P_{conv.add} = -h_{add} \cdot A_{cross.pad} \cdot (T_{hot} - T_{air})$$

If is true that $P_{cond.wire} = P_{conv.add}$, $T_{PCB} = T_{air}$ then equivalent of an additional heat convection coefficient can be calculated from the equation:

$$-k_{pyrex} \cdot \frac{A_{cross.wire}}{L_{wire}} = -h_{add} \cdot A_{cross.pad}$$

$$h_{add} = \frac{k_{pyrex}}{L_{wire}} \cdot \frac{A_{cross.wire}}{A_{cross.pad}}$$

Using the parameter values from table 1 we got:

$$h_{add} = \frac{318W/mK}{4 \cdot 10^{-3} m} \cdot \frac{\pi(12.5\mu m)^2}{(150\mu m)^2} \cong 1.7 \frac{kW}{m^2 K}$$

It can be estimated that heat drained through the wire-bonding connection is about 350 times higher than heat which goes out by the standard convection process over the pad surface. Hence, this heat draining effect definitively can't be neglected, on contrary its impact will be clearly seen on further temperature distribution analysis.

5. Simulation results

The most important simulation result is the temperature distribution on the sensor element: silicon die and pyrex support, shown in figure 4.

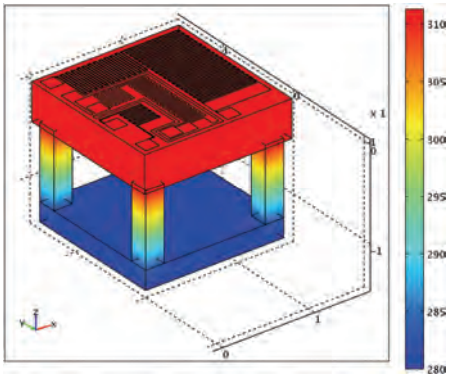

Figure 4. The external boundary temperature profile.

Directly from temperature profile (figure 4) can be observed temperature gradients occurring in the support pillars. It is also interesting to see the temperature profiles on the top and bottom die's surfaces illustrated in figures 5 and 6, where lateral gradients of temperature are clearly seen.

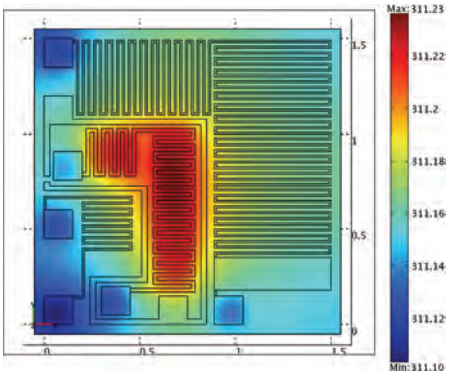

Figure 5. Temperature profile of the top surface of the silicon die with platinum resistances and gold pads.

7. Conclusions

Multiphysics FEM Simulation in COMSOL environment reveals that the entire silicon die has an almost uniform temperature. The hottest points of the die surface are due to the core of the heating resistor, whereas the coldest parts are located at the electrical pads, where electrical wire-bonding have been soldered connecting the hot die with the much colder PCB base. At the same time the temperature difference between the hottest and the coldest spots in the silicon die surface is just 0.13K. In comparison to the 30K of overheat this value is less than 0.5%, so for a global estimation model it can be neglected and assumed that temperature distribution is uniform.

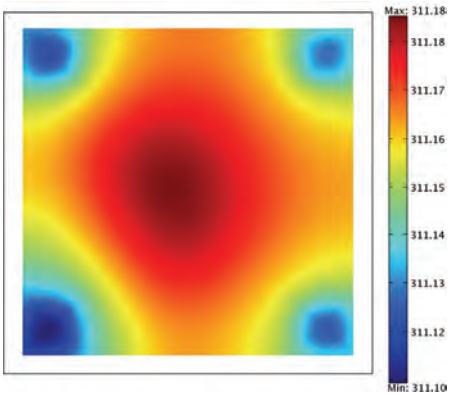

Figure 6. Temperature profile of the bottom surface of the silicon die with glued pyrex support structure.

8. References

1. J. Gómez-Elvira, at al. "Environmental monitoring instrument for Mars exploration", Lunar and Planetary Science 39, 2008, pp. 1647
2. L. Kowalski, et al. "Sensitivity analysis of the chip for REMS wind sensor", proceedings of the 7th Spanish Conference on Electron Devices, Feb 2009, ISBN: 978-1-4244-2838-0**,** pp. 289–292
3. M. Dominguez, et al. "A hot Film anemometer for the Martian atmosphere" Planetary and Space Science, February 2008, vol. 56, pp. 1169-1179
4. V. Jimenez, et al. "Applications of hot film anemometry to space missions" in Eurosensors XXII, September 2008, pp. 15-19
5. L. Kowalski, et al. "Thermal modelling of the chip for the REMS wind sensor", International Journal of numerical Modelling: Electronic networks, devices and fields, September 2009, vol. 10.1002/jnm.738, pp. 1-14

9. Acknowledgement

This work received support from the Commissioner for Universities and Research of the Department of Innovation, Universities and Company of the Generalitat de Catalunya and of European Social Fund, scholarship 2006FI00302.